JACS
JOURNAL OF THE AMERICAN CHEMICAL SOCIETY

Article

Corrole#Fullerene Dyads: Formation of Long-Lived Charge-Separated States in Nonpolar Solvents

Francis D#Souza, Raghu Chitta, Kei Ohkubo, Mariusz Tasior, Navaneetha K. Subbaiyan, Melvin E. Zandler, Maciek K. Rogacki, Daniel T. Gryko, and Shunichi Fukuzumi

J. Am. Chem. Soc., **2008**, 130 (43), 14263-14272 • DOI: 10.1021/ja804665y • Publication Date (Web): 07 October 2008

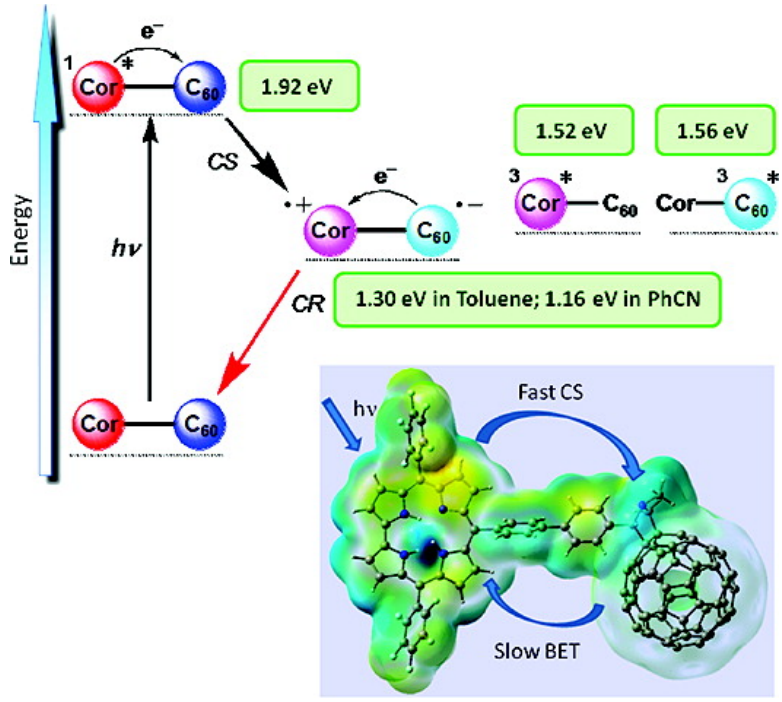

More About This Article

Additional resources and features associated with this article are available within the HTML version:

- Supporting Information
- Access to high resolution figures
- Links to articles and content related to this article
- Copyright permission to reproduce figures and/or text from this article

Journal of the American Chemical Society is published by the American Chemical Society. 1155 Sixteenth Street N.W., Washington, DC 20036

J|A|C|S
ARTICLES

Published on Web 10/07/2008

Corrole−Fullerene Dyads: Formation of Long-Lived Charge-Separated States in Nonpolar Solvents

Francis D'Souza,*,† Raghu Chitta,† Kei Ohkubo,‡ Mariusz Tasior,§ Navaneetha K. Subbaiyan,† Melvin E. Zandler,† Maciek K. Rogacki,§ Daniel T. Gryko,*,§ and Shunichi Fukuzumi*,‡

Department of Chemistry, Wichita State University, 1845 Fairmount, Wichita, Kansas 67260-0051, Department of Material and Life Science, Graduate School of Engineering, Osaka University, SORST, Japan Science and Technology Agency, Suita, Osaka 565-0871, Japan, and Institute of Organic Chemistry of the Polish Academy of Sciences, Kasprzaka 44/52, 01-224 Warsaw, Poland

Received June 18, 2008; E-mail: Francis.DSouza@wichita.edu; fukuzumi@chem.eng.osaka-u.ac.jp; Daniel@icho.edu.pl

Abstract: The first example of covalently linked free-base corrole−fullerene dyads is reported. In the newly synthesized dyads, the free-energy calculations performed by employing the redox and singlet excited-state energy in both polar and nonpolar solvents suggested the possibility of electron transfer from the excited singlet state of corrole to the fullerene entity. Accordingly, steady-state and time-resolved emission studies revealed efficient fluorescence quenching of the corrole entity in the dyads. Further studies involving femtosecond laser flash photolysis and nanosecond transient absorption studies confirmed electron transfer to be the quenching mechanism, in which the electron-transfer product, the fullerene anion radical, was able to be spectrally characterized. The rate of charge separation, k_{CS}, was found to be on the order of $10^{10}-10^{11}$ s^{-1}, suggesting an efficient photoinduced electron-transfer process. Interestingly, the rate of charge recombination, k_{CR}, was slower by 5 orders of magnitude in nonpolar solvents, cyclohexane and toluene, resulting in a radical ion-pair lasting for several microseconds. Careful analysis of the kinetic and thermodynamic data using the Marcus approach revealed that this novel feature is due to appropriately positioning the energy level of the charge-separated state below the triplet states of either of the donor and acceptor entities in both polar and nonpolar solvents, a feature that was not evident in donor−acceptor dyads constructed using symmetric tetrapyrroles as electron donors.

Introduction

Studies on artificial donor−acceptor constructs mimicking the primary events of natural photosynthesis lie at the heart of photosynthetic solar energy conversion and development of opto-electronic devices.[1−11] Several molecular and supramolecular dyads, triads, tetrads, etc. have been elegantly designed and studied with an emphasis on generating long-lived charge-separated states through a charge migration route, and for the construction of systems that are capable of performing "antenna-reaction center" events.[4−12] Systematic investigations probing the role of the photoactive unit (sensitizer), the nature of the electron acceptor, the spacer connecting the donor−acceptor entities, the spatial arrangement of the different entities, and the choice of secondary electron donor and acceptor in polyads have provided a wealth of information for direct utilization of

† Wichita State University.
‡ Osaka University.
§ Polish Academy of Sciences.

(1) (a) Sutin, N.; Brunschwig, B. S. *Adv. Chem. Ser.* **1990**, *226*, 65–88. (b) Bolton, J. R.; Mataga, N.; McLendon, G. *Adv. Chem. Ser.* **1991**, *228*, 295. (c) Wheeler, R. A. *Introduction to the Molecular Bioenergetics of Electron, Proton, and Energy Transfer*; ACS Symposium Series *883*, Molecular Bioenergetics; American Chemical Society: Washington, DC,2004; pp 1−6. (d) Leibl, W.; Mathis, P. Electron Transfer in Photosynthesis. In *Molecular to Global Photosynthesis*; Archer, M. D., Barber, J. Eds.; Photoconversion of Solar Energy *2*; Imperial College Press: London, 2004; p 117.

(2) (a) Kirmaier, C.; Holton, D. In *The Photosynthetic Reaction Center*; Deisenhofer, J., Norris, J. R. Eds.; Academic Press: San Diego, 1993; Vol. II, pp 49−70. (b) Balzani, V.; Juris, A.; Venturi, M.; Campagna, S.; Serroni, S. *Chem. Rev.* **1996**, *96*, 759–834.

(3) (a) Miller, J. R.; Calcaterra, L. T.; Closs, G. L. *J. Am. Chem. Soc.* **1984**, *106*, 3047–3049. (b) Closs, G. L.; Miller, J. R. *Science* **1988**, *240*, 440–447. (c) Connolly, J. S.; Bolton, J. R. In *Photoinduced Electron Transfer*; Fox, M. A., Chanon, M. Eds.; Elsevier: Amsterdam, 1988; Part D, pp 303−393.

(4) (a) Wasielewski, M. R. *Chem. Rev.* **1992**, *92*, 435–461. (b) Kurreck, H.; Huber, M. *Angew. Chem., Int. Ed. Engl.* **1995**, *34*, 849–866. (c) Gust, D.; Moore, T. A.; Moore, A. L. *Acc. Chem. Res.* **2001**, *34*, 40–48.

(5) (a) Sessler, J. S.; Wang, B.; Springs, S. L.; Brown, C. T. In *Comprehensive Supramolecular Chemistry*; Atwood, J. L., Davies, J. E. D., MacNicol, D. D. , Vögtle, F. Eds.; Pergamon: New York, 1996; Chapter 9. (b) Hayashi, T.; Ogoshi, H. *Chem. Soc. Rev.* **1997**, *26*, 355–364. (c) Ward, M. W. *Chem. Soc. Rev.* **1997**, *26*, 365–375.

(6) (a) BalzaniV.; Scandola, F. *Supramolecular Chemistry*; Ellis Horwood: New York, 1991. (b) Schlicke, B.; De Cola, L.; Belser, P.; Balzani, V. *Coord. Chem. Rev.* **2000**, *208*, 267–275. (c) de Silva, A. P.; Gunaratne, H. Q. N.; Gunnlaugsson, T.; Huxley, A. J. M.; Mccoy, C. P.; Rademacher, J. T.; Rice, T. E. *Adv. Supramol. Chem.* **1997**, *4*, 1–53. (d) Ashton, P. R.; Ballardini, R.; Balzani, V.; Credi, A.; Dress, K. R.; Ishow, E.; Kleverlaan, C. J.; Kocian, O.; Preece, J. A.; Spencer, N.; Stoddart, J. F.; Venturi, M.; Wenger, S. *Chem. Eur. J,* **2000**, *6*, 3558–3574.

(7) (a) Aviram, A.; Ratner, M. *Ann. N.Y. Acad. Sci.* **1998**, 852. (b) *Molecular Switches*; Feringa, B. L. Ed.;Wiley-VCH GmbH: Weinheim, 2001. (c) Gust, D.; Moore, T. A.; Moore, A. L. *Chem. Commun.* **2006**, 1169–1178.

these systems for the aforementioned applications.[4−12] Owing to its resemblance to the natural photosynthetic chlorophyll pigment and relatively easy synthetic manipulations, porphyrin as the primary photoactive entity has dominated this area of research.[9−12] Additionally, several porphyrin-like molecules with interesting photo- and redox properties, viz., phthalocyanines,[13] naphthalocyanines,[14] subphthalocyanines,[15] chlorins,[16] *N*-confused porphyrins,[17] and fused porphyrins,[18] have also been successfully utilized in the construction of donor−acceptor systems. In several instances, valuable information which is otherwise not attainable using traditional porphyrins has been obtained.[13−18] As the choice of the electron acceptor, fullerene (C_{60})[19] has dominated the field compared to any other electron-acceptor, including quinones, in recent years. This is because of its three-dimensional structure, reduction potential comparable to that of benzoquinone, strong absorption in the UV−visible region,[20] and importantly, small reorganization energy in electron-transfer reactions.[21]

According to Marcus theory,[22] a slow charge recombination process is theoretically attainable by lowering the solvent reorganization energy. Fullerene has served as an excellent example to verify this prediction in polar solvent media.[11,21] Alternatively, one could observe such a phenomenon by lowering the polarity of the solvent media, which would effectively increase the free-energy change associated with the charge recombination process.[23] However, in the majority of donor−fullerene linked systems constructed using symmetric tetrapyrroles, such as porphyrin and phthalocyanine, it was often difficult to probe a slower charge recombination process in nonpolar solvents.[24] This is because the energy of the charge-separated state was higher than the triplet excited energy of either of the electron donor and acceptor entities.[24] Consequently, population of the triplet excited state instead of direct charge recombination to the ground state was observed for these dyads in nonpolar solvents. It should be noted that the protein environment surrounding the photosynthetic reaction center is nonpolar, with a low dielectric constant (ϵ) of ca. 2.[25] Thus, it is desired to develop donor−acceptor dyads which can afford long-lived charge-separated states in nonpolar media.

Corroles, one-carbon-shorter analogues of porphyrins, emerged a few years ago as an independent area of research.[26] First reported in 1965,[27] they possess the skeleton of corrin (macrocycle found in vitamin B_{12}) with three *meso*-carbons between the four pyrrole rings. Recent synthetic breakthroughs have made these macrocycles readily available.[28] When compared with porphyrins, these tribasic aromatic macrocycles exhibit interest-

(8) (a) *Supramolecular Chemistry*; Atwood, J. L., Davies, J. E. D., MacNicol, D. D., Vögtle, F., Reinhoudt, D. N. Eds.; Pergamon: Oxford, 1996; Vol. 10, pp171−185. (b) Dickert, F. L.; Haunschild, A. *Adv. Mater.* **1993**, *5*, 887–895. (c) Schierbaum, K. D.; Göpel, E. *Synth. Met.* **1993**, *61*, 37–45. (d) de Silva, A. P.; Gunaratne, H. Q. N.; Gunnlaugsson, T.; Huxley, A. J. M.; McCoy, C. P.; Rademacher, J. T.; Rice, T. E. *Chem. Rev.* **1997**, *97*, 1515–1566. (e) Lehn, J.-M. *Front. Supramol. Org. Chem. Photochem.* **1991**, 1–28. (f) Bell, T. W.; Hext, N. M. *Chem. Soc. Rev.* **2004**, *33*, 589–598.

(9) (a) Gust, D.; Moore, T. A. In *The Porphyrin Handbook*; Kadish, K. M., Smith, K. M., Guilard, R. Eds.; Academic Press: Burlington, MA, 2000; Vol. 8, pp 153−190. (b) Prato, M. *J. Mater. Chem.* **1997**, *7*, 1097–1109. (c) Martín, N.; Sánchez, L.; Illescas, B.; Pérez, I. *Chem. Rev.* **1998**, *98*, 2527–2547. (d) Diederich, F.; Gómez-López, M. *Chem. Soc. Rev.* **1999**, *28*, 263–277.

(10) (a) Imahori, H.; Sakata, Y. *Adv. Mater.* **1997**, *9*, 537–546. (b) Guldi, D. M. *Chem. Commun.* **2000**, 321–327. (c) Guldi, D. M.; Prato, M. *Acc. Chem. Res.* **2000**, *33*, 695–703. (d) Guldi, D. M. *Chem. Soc. Rev.* **2002**, *31*, 22–36. (e) Meijer, M. E.; van Klink, G. P. M.; van Koten, G. *Coord. Chem. Rev.* **2002**, *230*, 141–163. (f) El-Khouly, M. E.; Ito, O.; Smith, P. M.; D'Souza, F. *J. Photochem. Photobiol. C* **2004**, *5*, 79–104. (g) Imahori, H.; Fukuzumi, S. *Adv. Funct. Mater.* **2004**, *14*, 525–536. (h) D'Souza, F.; Ito, O. *Coord. Chem. Rev.* **2005**, *249*, 1410–1422. (i) Sanchez, L.; Martin, N.; Guldi, D. M. *Angew. Chem., Int. Ed.* **2005**, *44*, 5374–5382. (j) Bouamaied, T. I.; Coskun, E. S. *Struct. Bonding (Berlin)* **2006**, *121*, 1–147.

(11) (a) Imahori, H.; Tamaki, K.; Guldi, D. M.; Luo, C.; Fujitsuka, M.; Ito, O.; Sakata, Y.; Fukuzumi, S. *J. Am. Chem. Soc.* **2001**, *123*, 2607–2617. (b) Imahori, H.; Guldi, D. M.; Tamaki, K.; Yoshida, Y.; Luo, C.; Sakata, Y.; Fukuzumi, S. *J. Am. Chem. Soc.* **2001**, *123*, 6617–6628. (c) Imahori, H.; Sekiguchi, Y.; Kashiwagi, Y.; Sato, T.; Araki, Y.; Ito, O.; Yamada, H.; Fukuzumi, S. *Chem.-Eur. J.* **2004**, *10*, 3184–3196. (d) Tanaka, M.; Ohkubo, K.; Gros, C. P.; Guilard, R.; Fukuzumi, S. *J. Am. Chem. Soc.* **2006**, *128*, 14625–14633.

(12) (a) Fukuzumi, S. *Phys. Chem. Chem. Phys.* **2008**, *10*, 2283–2297. (b) Chitta, R.; D'Souza, F. *J. Mater. Chem.* **2008**, *18*, 1440–1471. (c) Fukuzumi, S.; Kojima, T. *J. Mater. Chem.* **2008**, *18*, 1427–1439.

(13) (a) Li, X.; Sinks, L. E.; Rybtchinski, B.; Wasielewski, M. R. *J. Am. Chem. Soc.* **2004**, *126*, 10810–10811. (b) Guldi, D. M.; Zilbermann, I.; Gouloumis, A.; Vazquez, P.; Torres, T. *J. Phys. Chem. B* **2004**, *108*, 18485–18494. (c) Fukuzumi, S.; Ohkubo, K.; Ortiz, J.; Gutiérrez, A. M.; Fernández-Lázaro, F.; Sastre-Santos, Á. *Chem. Commun.* **2005**, 3814–3816. (d) Jiménez, Á. J.; Spänig, F.; Rodríguez-Morgade, M. S.; Ohkubo, K.; Fukuzumi, S.; Guldi, D. M.; Torres, T. *Org. Lett.* **2007**, *9*, 2481–2484.

(14) El-Khouly, M. E.; Rogers, L. M.; Zandler, M. E.; Suresh, G.; Fujitsuka, M.; Ito, O.; D'Souza, F. *ChemPhysChem* **2003**, *4*, 474–481.

(15) (a) González-Rodríguez, D.; Torres, T.; Guldi, D. M.; Rivera, J.; Herranz, M. Á.; Echegoyen, L. *J. Am. Chem. Soc.* **2004**, *126*, 6301–6313. (b) González-Rodríguez, D.; Claessens, C. G.; Torres, T.; Liu, S. G.; Echegoyen, L.; Vila, N.; Nonell, S. *Chem.-Eur. J.* **2005**, *11*, 3881–3893.

(16) (a) Balaban, T. S.; Tamiaki, H. R.; Holzwarth, A. In *Supramolecular Dye Chemistry*; Würthner, F. Ed.; Topics in Current Chemistry *258*; Springer: Berlin, 2005; pp1−38. (b) Balaban, T. S. *Acc. Chem. Res.* **2005**, *38*, 612–623. (c) Huber, V.; Katterle, M.; Lysetska, M.; Würthner, F. *Angew. Chem., Int. Ed.* **2005**, *44*, 3147–3151. (d) Sasaki, S.; Mizoguchi, T.; Tamiaki, H. *Tetrahedron* **2005**, *61*, 8041–8048. (e) Kelley, R. F.; Tauber, M. J.; Wasielewski, M. R. *J. Am. Chem. Soc.* **2006**, *128*, 4779–4791. (f) Röger, C.; Müller, M. G.; Lysetska, M.; Miloslavina, Y.; Holzwarth, A. R.; Würthner, F. *J. Am. Chem. Soc.* **2006**, *128*, 6542–6543. (g) Fukuzumi, S.; Ohkubo, K.; Imahori, H.; Shao, J.; Ou, Z.; Zheng, G.; Chen, Y.; Pandey, R. K.; Fujitsuka, M.; Ito, O.; Kadish, K. M. *J. Am. Chem. Soc.* **2001**, *123*, 10676–10683. (h) Ohkubo, K.; Kotani, H.; Shao, J.; Ou, Z.; Kadish, K. M.; Li, G.; Pandey, R. K.; Fujitsuka, M.; Ito, O.; Imahori, H.; Fukuzumi, S. *Angew. Chem., Int. Ed.* **2004**, *43*, 853–856.

(17) D'Souza, F.; Smith, P. M.; Rogers, L.; Zandler, M. E.; Shafiqul Islam, D.-M.; Araki, Y.; Ito, O. *Inorg. Chem.* **2006**, *45*, 5057–5065.

(18) (a) Mataga, N.; Taniguchi, S.; Chosrowjan, H.; Osuka, A.; Yoshida, N. *Photochem. Photobiol. Sci.* **2003**, *2*, 493–500. (b) Hwang, I. W.; Kamada, T.; Ahn, T. K.; Ko, D. M.; Nakamura, T.; Tsuda, A.; Osuka, A.; Kim, D. *J. Am. Chem. Soc.* **2004**, *126*, 16187–16198. (c) Kashiwagi, Y.; Ohkubo, K.; McDonald, J. A.; Blake, I. M.; Crossley, M. J.; Araki, Y.; Ito, O.; Imahori, H.; Fukuzumi, S. *Org. Lett.* **2003**, *5*, 2719–2721.

(19) For review papers on this topic, see the special issue on Fullerene: *C. R. Chem.* **2006**, *9*, issues 7 and 8.

(20) (a) Kroto, H. W.; Heath, J. R.; O'Brien, S. C.; Curl, R. F.; Smalley, R. E. *Nature* **1985**, *318*, 162–163. (b) Kratschmer, W.; Lamb, L. D.; Fostiropoulos, F.; Huffman, D. R. *Nature* **1990**, *347*, 354–358. (c) *Fullerene and Related Structures*; Hirsch, A. Eds.; Springer: Berlin, 1999; Vol. 199. (d) Allemand, P. M.; Koch, A.; Wudl, F.; Rubin, Y.; Diederich, F.; Alvarez, M. M.; Anz, S. J.; Whetten, R. L. *J. Am. Chem. Soc.* **1991**, *113*, 1050–1051. (e) Xie, Q.; Perez-Cordero, E.; Echegoyen, L. *J. Am. Chem. Soc.* **1992**, *114*, 3978–3980.

(21) (a) Fukuzumi, S.; Nakanishi, I.; Suenobu, T.; Kadish, K. M. *J. Am. Chem. Soc.* **1999**, *121*, 3468–3474. (b) Fukuzumi, S.; Ohkubo, K.; Imahori, H.; Guldi, D. M. *Chem.-Eur. J.* **2003**, *9*, 1585–1593. (c) Imahori, H.; El-Khouly, M. E.; Fujitsuka, M.; Ito, O.; Sakata, Y.; Fukuzumi, S. *J. Phys. Chem. A* **2001**, *105*, 325–332.

(22) (a) Marcus, R. A.; Sutin, N. *Biochim. Biophys. Acta* **1985**, *811*, 265–322. (b) Marcus, R. A. *Angew. Chem., Int. Ed. Engl.* **1993**, *32*, 1111–1121.

(23) Fukuzumi, S.; Ohkubo, K.; E, W.; Ou, Z.; Shao, J.; Kadish, K. M.; Hutchison, J. A.; Ghiggino, K. P.; Sintic, P. J.; Crossley, M. J. *J. Am. Chem. Soc.* **2003**, *125*, 14984–14985.

(24) Imahori, H.; El-Khouly, M. E.; Fujitsuka, M.; Ito, O.; Sakata, Y.; Fukuzumi, S. *J. Phys. Chem. A* **2001**, *105*, 325–332.

(25) (a) Hutter, M. C.; Hughes, J. M.; Reimers, J. R.; Hush, N. S. *J. Phys. Chem. B* **1999**, *103*, 4906–4915. (b) Harvey, S. C. *Proteins* **1989**, *5*, 78–92.

Chart 1

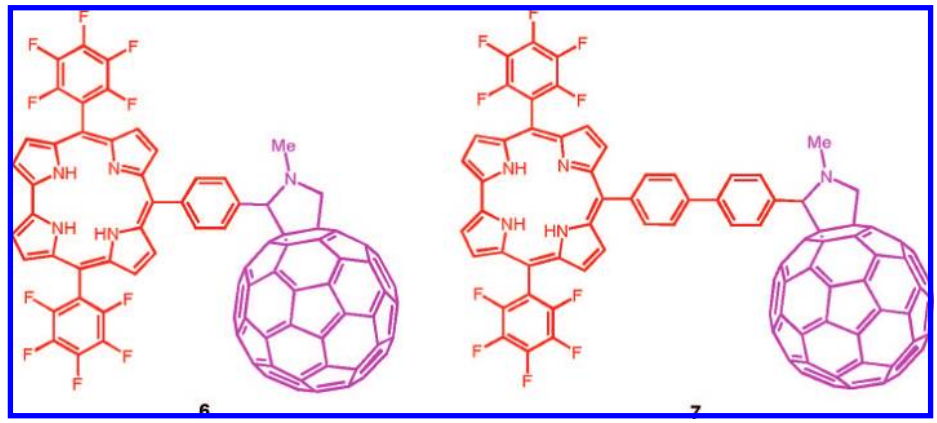

ing properties, including lower oxidation potentials, higher fluorescence quantum yields, larger Stokes shift, and relatively more intense absorption of red light.[29] Although less stable compared to analogous porphyrins, assemblies of appropriately functionalized corroles with other redox-active and photoactive moieties for different applications have recently emerged.[30] Redox and spectroscopic properties of corroles suggest that covalently attaching a well-known electron acceptor such as fullerene might lead to dyads with novel photochemical and photophysical properties.This has been explored in the present study by covalently linking free-base corrole to a fullerene entity to form new series of donor−acceptor dyads (Chart 1).

In the newly synthesized dyads, a phenyl or a biphenyl spacer unit has been employed to probe the role of distance between the donor and acceptor entities in electron-transfer reactions (Chart 1). The intentionally chosen two *meso*-pentafluorophenyl entities fulfill two functions. First, they stabilize the rather less stable corrole macrocycle, and second, being electron-withdrawing, they suitably position the energy level of the charge-separated state to achieve long-lived radical ion-pairs in nonpolar solvents (*vide infra*). As demonstrated here, dyads **6** and **7** undergo efficient photoinduced electron transfer from the singlet excited corrole to fullerene and a slow charge recombination process in nonpolar solvents. Careful examination of the kinetic and thermodynamic data in relation to Marcus theory demonstrates that the energy level of the charge-separated state is lower than the triplet energy level of either of the corrole and fullerene entities, a novel feature that was not evident in donor−acceptor dyads constructed using symmetric tetrapyrroles as electron donors.

Results and Discussion

Synthesis and Spectroscopy. The corrole−fullerene dyads in the present study were designed to visualize the effect of donor−acceptor distance and the resulting intramolecular interactions on the rates of charge separation and charge recombination. With this in mind, rigid phenylene and biphenylene spacers were introduced between the donor and acceptor entities. Additionally, two electron-withdrawing substituents at the 5 and 15 positions of the *trans*-A_2B type corrole core were introduced to attain higher stability of the macrocycle and a suitable energy state for charge separation (*vide infra*). For the construction of the necessary building block (corroles **4** and **5**, Scheme 1), the newest method[31] was chosen, which proved suitable for preparation of various 10-(formylaryl)-corroles via the direct condensation of aromatic dialdehydes with dipyrromethanes.[32] Consequently, synthesis of the dyad involved two steps. Reaction of 5-pentafluorophenyldipyrromethane (**1**) with a given dialdehyde (**2**, **3**) led directly to corroles **4** and **5** possessing a free formyl group in ∼30% yields. Subsequently, corroles **4** and **5** were subjected to the standard Prato method of fulleropyrrolidine synthesis[33] (C_{60} and sarcosine) to furnish dyads **6** and **7** in ∼40% yield (Scheme 1). The structural integrity of the newly synthesized dyads was established from ^{1}H NMR, MALDI-mass, spectral, and electrochemical methods (see Experimental Section).

The optical absorption spectrum of the corrole−fullerene dyad **6** and a corrole reference compound (**4**) in toluene is shown in

(26) (a) Paolesse, R. In *The Porphyrin Handbook*; Kadish, K. M., Smith, K. M., Guilard, R. Eds.; Academic Press: New York, 2000; Vol. 2, pp 201−232. (b) Gryko, D. T.; Fox, J. P.; Goldberg, D. P. *J. Porphyrins Phthalocyanines* **2004**, *8*, 1091–1105. (c) Guilard, R.; Barbe, J.-M.; Stern, C.; Kadish, K. M. In *The Porphyrin Handbook*; Kadish, K. M., Smith, K. M., Guilard, R. Eds.; Elsevier Science: New York, Vol. 18, pp 303−351. (d) Aviv, I.; Gross, Z. *Chem. Commun.* **2007**, *20*, 1987–1999. (e) Nardis, S.; Monti, D.; Paolesse, R. *Mini-Rev. Org. Chem.* **2005**, *2*, 355–372.
(27) Johnson, A. W.; Kay, I. T. *J. Chem. Soc.* **1965**, 1620–1629.
(28) (a) Vogel, E.; Will, S.; Shulze-Tilling, A.; Neumann, L.; Lex, J.; Bill, E.; Trautwein, A. X.; Wieghardt, K. *Angew. Chem., Int. Ed. Engl.* **1994**, *33*, 731–734. (b) Gross, Z.; Galili, N.; Saltsman, I. *Angew. Chem., Int. Ed.* **1999**, *38*, 1427–1429. (c) Paolesse, R.; Jaquinod, L.; Nurco, D. J.; Mini, S.; Sagone, F.; Boschi, T.; Smith, K. M. *Chem. Commun.* **1999**, 1307–1308. (d) Gryko, D. T. *Eur. J. Org. Chem.* **2002**, 1735–1742.
(29) (a) Ding, T.; Alemán, E. A.; Mordarelli, D. A.; Ziegler, C. J. *J. Phys. Chem. A* **2005**, *109*, 7411–7417. (b) Ventura, B.; Degli Esposti, A.; Koszarna, B.; Gryko, D. T.; Flamigni, L. *New J. Chem.* **2005**, *29*, 1559–1566. (c) Bendix, J.; Dmochowski, I. J.; Gray, H. B.; Mahammed, A.; Simkhovic, L.; Gross, Z. *Angew. Chem., Int. Ed.* **2000**, *39*, 4048–4051. (d) Poulin, J.; Stern, C.; Guilard, R.; Harvey, D. *Photochem. Photobiol.* **2006**, *82*, 171–176. (e) Van der Boom, T.; Hayes, R. T.; Zhao, Y.; Bushard, P. J.; Weiss, E. A.; Wasielewski, M. R. *J. Am. Chem. Soc.* **2002**, *124*, 9582–9590. (f) Tomizaki, K.; Loewe, R. S.; Kirmaier, C.; Scwartz, J. K.; Retsek, J. L.; Bocian, D. F.; Holten, D.; Lindsey, J. S. *J. Org. Chem.* **2002**, *67*, 6519–6534. (g) Okamoto, K.; Mori, Y.; Yamada, H.; Imahori, H.; Fukuzumi, S. *Chem.-Eur. J.* **2004**, *10*, 474–483.
(30) (a) Tasior, M.; Gryko, D. T.; Cembor, M.; Jaworski, J. S.; Ventura, B.; Flamigni, L. *New J. Chem.* **2007**, *31*, 247–259. (b) Flamigni, L.; Ventura, B.; Tasior, M.; Gryko, D. T. *Inorg. Chim. Acta* **2007**, *360*, 803–813. (c) Flamigni, L.; Ventura, B.; Tasior, M.; Becherer, T.; Langhals, H.; Gryko, D. T. *Chem. Eur. J.* **2008**, *14*, 169–183. (d) Gros, C. P.; Brisach, F.; Meristoudi, A.; Espinosa, E.; Guillard, R.; Harvey, P. D. *Inorg. Chem.* **2007**, *46*, 125–135.
(31) Koszarna, B.; Gryko, D. T. *J. Org. Chem.* **2007**, *71*, 3707–3717.
(32) Gryko, D. T.; Piechowska, J.; Jaworski, J. S.; Gałęzowski, M.; Tasior, M.; Cembor, M.; Butenschön, H. *New J. Chem.* **2007**, *31*, 1613–1619.
(33) Maggini, M.; Scorrano, G.; Prato, M. *J. Am. Chem. Soc.* **1993**, *115*, 9798–9799.

Scheme 1

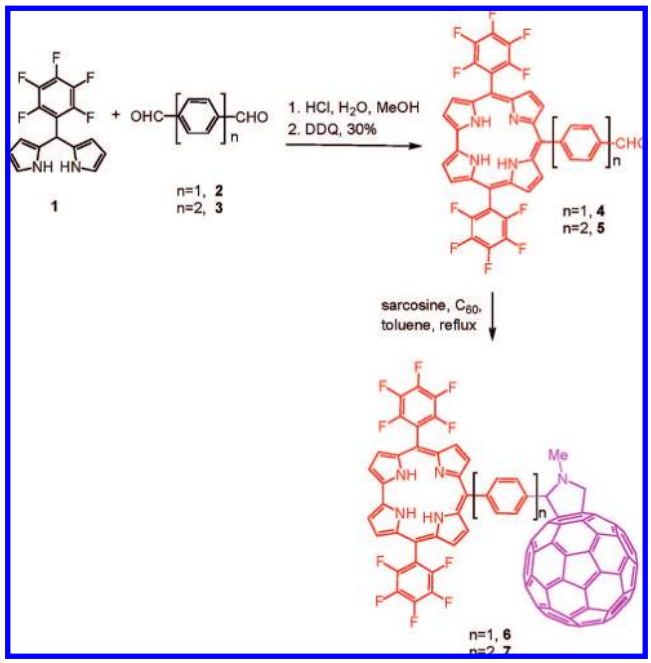

Figure 1. The dyad **6** revealed a band around 310 nm corresponding to the fulleropyrrolidine entity. The Soret band of the dyad was blue-shifted by 5 nm compared to the reference corrole bearing an aldehyde group instead of fullerene. Such a trend was also observed for the visible band located around 560 nm; however, the blue-shift was around 2 nm. No new bands in the near-IR portion from 750 to 1100 nm were observed for these dyads.The blue-shifted Soret and visible bands suggest electronic interactions between the corrole and fullerene entities of the dyad. Similar spectral observations were also made for dyad **7**. That is, peaks corresponding to both the corrole and fullerene entities and slightly blue-shifted spectral bands were noticed.

DFT B3LYP/3-21G(*) Calculations. To visualize the geometry and electronic structure of the dyads, computational studies were performed at the DFT B3LYP/3-21G(*) level.[34,35] For this, the dyads were optimized on a Born−Oppenheimer potential energy surface, and a global minimum for each dyad was obtained. The structure of the energy-optimized dyad **6** is shown in Figure 2a, in which closely disposed corrole and fullerene entities were recognized. That is, the edge-to-edge distance from the corrole ring carbon to the nearest C_{60} carbon was estimated to be 5.1 Å, while the center-to-center distance (R_{ct-ct}) between them was estimated to be 12.5 Å. The molecular electrostatic potential (MEP) map calculated at the B3LYP/3-21G(*) level is shown in Figure 2b. The positive electrostatic potential of fulleropyrrolidine was at the pyrrolidine ring, while the negative electrostatic potential was spread over the fullerene spheroid. For the free-base corrole, the negative potential was mainly associated with the pyrrole rings of the macrocycle and the *meso*-aromatic substituents, while the positive potential was on the inner imino groups.The B3LYP/3-21G(*)-generated frontier highest occupied molecular orbital (HOMO) and lowest unoccupied molecular orbital (LUMO) are shown in Figure 2c,d. The HOMO was located on the corrole π-system, while the LUMO was located on the fullerene spheroid. Importantly, part of the HOMO was also on the *meso*-phenylene spacer of the dyad, suggesting considerable interaction between the donor and acceptor entities.[36] The locations of the HOMO and LUMO also suggest formation of a corrole$^{\bullet+}$−$C_{60}^{\bullet-}$ charge-separated state during photoinduced electron transfer.

Owing to the presence of a biphenyl spacer in the case of dyad **7**, an increased donor−acceptor distance and less spreading of the HOMO were observed (see Figure S1 in the Supporting Information). As expected, the phenyl rings of the biphenyl spacer unit attained a twisted configuration in the optimized structure of **7**. The calculated center-to-center distances for the dyads are listed in Table 1. The calculated gas-phase HOMO−LUMO

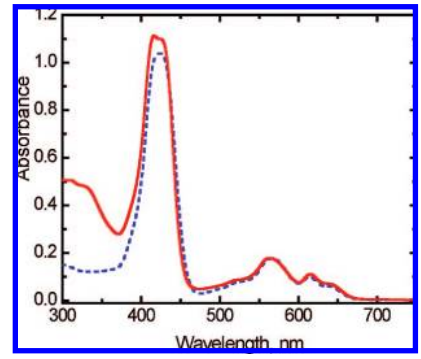

Figure 1. UV−visible absorption spectra of (a) corrole−fullerene dyad **6** (red solid line) and (b) corrole reference compound **4** (blue dashed line) in toluene.

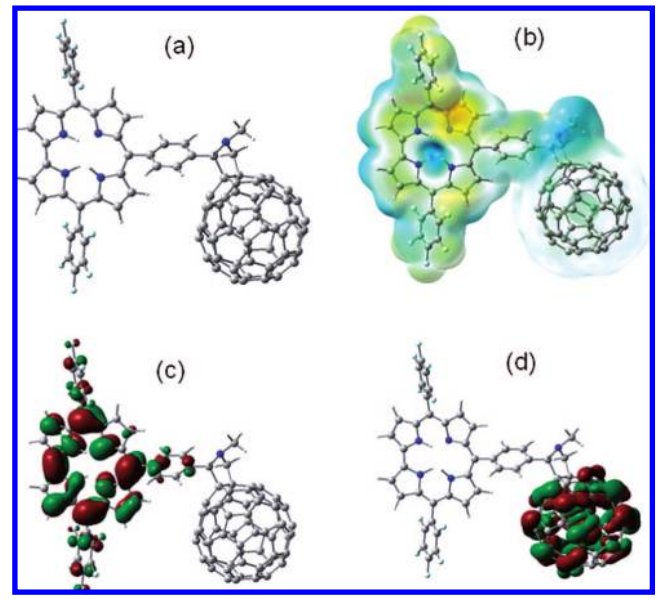

Figure 2. B3LYP/3-21G(*)-calculated (a) optimized structure, (b) molecular electrostatic potential map, (c) frontier HOMO, and (d) frontier LUMO of the corrole−fullerene dyad **6**. The red and blue colors in (b) indicate the negative and positive electrostatic potentials.

(34) Frisch, M. J., et al. *Gaussian 03*; Gaussian, Inc.: Pittsburgh, PA; 2003.

(35) For a general review on DFT applications of porphyrin−fullerene systems, see: Zandler, M. E.; D'Souza, F. *C. R. Chemie* **2006**, *9*, 960–981.

(36) (a) D'Souza, F.; Gadde, S.; Zandler, M. E.; Arkady, K.; El-Khouly, M. E.; Fujitsuka, M.; Ito, O. *J. Phys. Chem. A* **2002**, *106*, 12393–12404. (b) El-Khouly, M. E.; Araki, Y.; Ito, O.; Gadde, S.; McCarty, A. L.; Karr, P. A.; Zandler, M. E.; D'Souza, F. *Phys. Chem. Chem. Phys.* **2005**, *7*, 3163–3171. (c) D'Souza, F.; Maligaspe, E.; Karr, P. A.; Schumacher, A. L.; Oijami, M. L.; Gros, C. P.; Barbe, J.-M.; Ohkubo, K.; Fukuzumi, S. *Chem. Eur. J.* **2008**, *14*, 674–681.

Table 1. Electrochemical Redox Potentials (V vs Fc/Fc^+) and Free-Energy Changes for Backward Electron Transfer (ΔG_{BET}) and Charge Separation (ΔG_{CS}) for the Corrole−Fullerene Dyads in Different Solvents

R_{ct-ct}, Å	solvent	dielectric constant (ϵ)	$E_{ox}(Cor^{0/\bullet+})$, V	$E_{red}(C_{60}^{0/\bullet-})$, V	$-\Delta G_{BET}$,[a] eV	$-\Delta G_{CS}$,[b] eV
			Dyad **6**			
12.5	PhCN	25.9	0.18	−1.00	1.18	0.74
	THF	7.5	0.17	−0.95	1.12	0.80
	toluene	2.4	0.31	−0.99	1.30	0.62
			Dyad **7**			
16.7	PhCN	25.9	0.17	−1.00	1.17	0.75
	THF	7.5	0.17	−0.96	1.13	0.79
	toluene	2.4	0.28	−0.99	1.28	0.64

[a] ΔG_{BET} (in eV) $= e(E_{ox} - E_{red})$. [b] $-\Delta G_{CS} = \Delta E_{0-0} - (-\Delta G_{BET})$, where ΔE_{0-0} is the energy of the lowest excited state of free-base corrole. Error in potential $= \pm 0.02$ V.

gap was found to range between 1.72 and 1.77 eV for the dyads and is smaller than that reported in the literature for covalently linked porphyrin−fullerene dyads at the same computational level.[36a]

Redox Potentials and Free-Energies of Electron Transfer. Electrochemical studies using differential pulse voltammetry (DPV) were performed to evaluate the oxidation and reduction potentials and the experimental HOMO−LUMO gap of the newly synthesized dyads. Figure 3 shows DPVs of the representative dyad **6** in the studied solvents; the peak potentials for both of the dyads are listed in Table 1. Owing to the low dielectric constant of toluene, the DPVs were recorded in 0.5 M $(n\text{-hexyl})_4NClO_4$ at an elevated temperature of 313 K. In these solvents, the corrole unit exhibited up to four oxidations and two reductions,[37] while up to three one-electron reductions corresponding to the reduction of the fulleropyrrolidine[36] within the potential window of the solvent were observed. However, only the first oxidation of corrole and the first reduction of fullerene, needed to evaluate the free-energy change associated with photoinduced electron transfer in the dyad, were monitored in the present study. The oxidation potential of the corrole entity in these dyads was found to be solvent dependent, while such an effect on the fulleropyrrolidine reduction was found to be relatively small. That is, going from benzonitrile to toluene, the potential difference for oxidation of corrole was 140 mV, while the corresponding difference for fullerene reduction was 50 mV. It is also important to note that the corrole entity was easier to oxidize, based on comparison with the oxidation potentials of traditionally employed free-base and zinc porphyrins in building donor−acceptor dyads,[36a,b] in spite of the present corrole macrocycle possessing two pentafluorophenyl rings at the *meso*-positions of the macrocycle ring. The experimental HOMO−LUMO gap (potential difference between the first oxidation and the first reduction) was also found to be solvent dependent. That is, a smaller HOMO−LUMO gap was observed in polar benzonitrile solvent (Table 1).

The free-energy change associated with photoinduced electron transfer from the singlet excited corrole to fullerene ($-\Delta G_{CS}$), yielding the radical ion-pair $corrole^{\bullet+}-C_{60}^{\bullet-}$, and the free-energy change for charge recombination ($-\Delta G_{BET}$) from the radical ion-pair $corrole^{\bullet+}-C_{60}^{\bullet-}$, yielding neutral dyad in the ground state, calculated according to Rehm and Weller's approach,[38] are also listed in Table 1. The magnitude of ΔG_{CS} and ΔG_{BET} indicates photoinduced electron transfer, and the charge recombination reactions are thermodynamically favorable for the dyads while being solvent dependent to an appreciable extent.

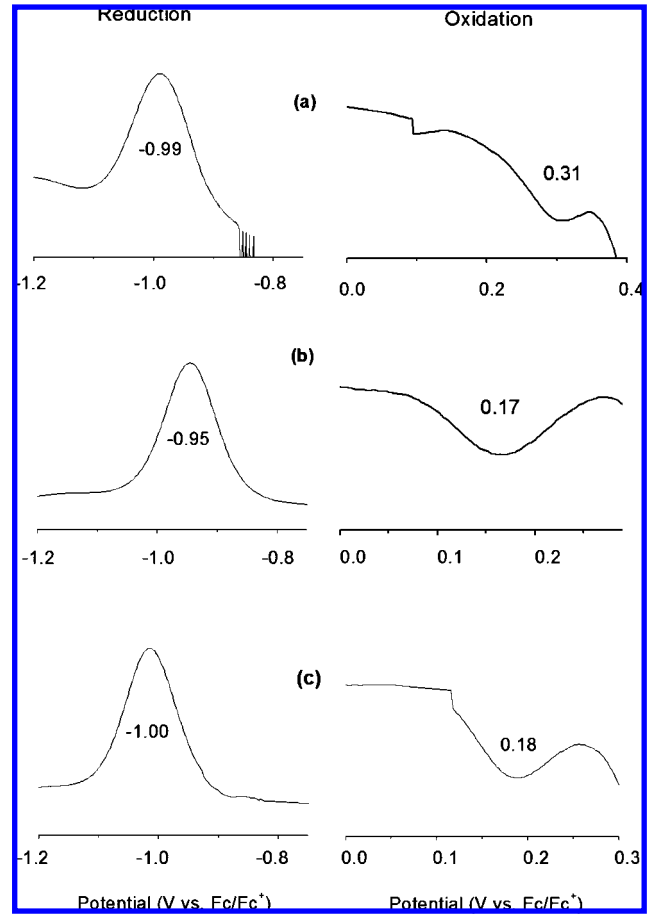

Figure 3. Differential pulse voltammograms showing the first reduction, corresponding to fulleropyrrolidine, and the first oxidation, corresponding to corrole, of the corrole−fullerene dyad **6** (a) in toluene containing 0.5 M $(n\text{-hexyl})_4NClO_4$ at 313 K, (b) in THF containing 0.1 M $(n\text{-}C_4H_9)_4NClO_4$ at 298 K, and (c) in benzonitrile containing 0.1 M $(n\text{-}C_4H_9)_4NClO_4$ at 298 K. Scan rate = 20 mV/s, pulse amplitude = 0.025 V, pulse duration = 50 ms, step time = 100 ms, step height = 2.0 mV. The concentration of the dyad was ∼0.1 mM.

Photoinduced Electron Transfer. Free-base corroles revealed an emission band located around 656 nm with a shoulder around 714 nm (Figure 4a, plot ii).[30] For both dyads, these emission bands were found to be fully quenched (over 97%) (Figure 4a, plot i). Changing the excitation wavelength to the Soret or visible region had no significant effect on the emission behavior of the dyads. These results indicate efficient excited-state events in the dyads. Generally, the quenching was greater in polar solvents (∼99%) compared to that in nonpolar solvents (∼97%). The low-temperature phosphorescence spectrum of corrole revealed a band at 818 nm, yielding a triplet excited energy of 1.52 eV (see Supporting Information, Figure S5, for the spectrum). These results suggest that the charge-separated state is lower in energy (see Table 1 for the data) compared to the

(37) Shen, J.; Shao, J.; Ou, Z.; E, W.; Koszarna, B.; Gryko, D. T.; Kadish, K. M. *Inorg. Chem.* **2006**, *45*, 2251–2265.

(38) (a) Rehm, D.; Weller, A. *Isr. J. Chem* **1970**, *7*, 259. (b) Mataga, N.; Miyasaka, H. In *Electron Transfer*; Jortner, J., Bixon, M. Eds.; John Wiley & Sons: New York, 1999; Part *2*, pp 431−496.

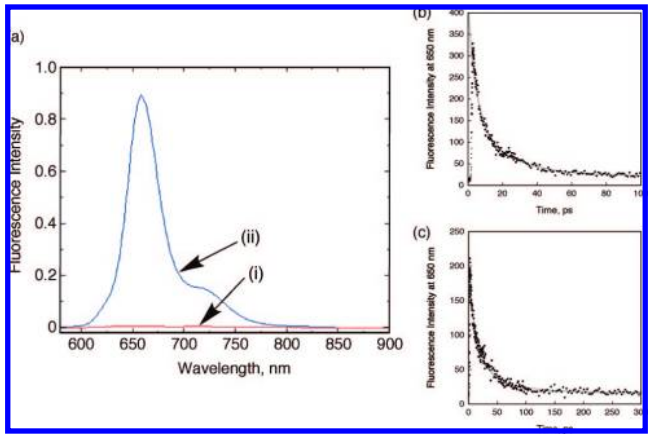

Figure 4. (a) Steady-state fluorescence spectra of (i) the corrole−fullerene dyad **6** and (ii) the corrole reference compound **4** in toluene. The concentrations were held at 5 μM, and the samples were excited at 562 nm. (b,c) Time-resolved fluorescence decay of the corrole−fullerene dyad **6** in (b) benzonitrile and (c) toluene. The samples were excited at λ_{ex} = 410 nm, and the emission was collected at λ_{em} = 650 nm. The solid curves represent the best fit to the two-exponential decay.

Table 2. Fluorescence Lifetime, Charge Separation Rate Constant (k_{CS}), Charge Recombination Rate Constant (k_{CR}), and Lifetime of the Radical Ion-Pair (τ_{RIP}) for the Corrole−Fullerene Dyads in Different Solvents

solvent	dielectric constant (ϵ)	fluorescence lifetime, ps	k_{CS}, s^{-1} [a]	k_{CR}, s^{-1} [b]	τ_{RIP}, ns
		Dyad **6**			
PhCN	25.9	4.5 (67%), 23 (33%)	2.2×10^{11}, 4.3×10^{10}	2.2×10^{10}	0.045
THF	7.5	5.0 (98%)	2.0×10^{11}	2.6×10^{10}	0.038
toluene	2.4	17 (97%)	5.9×10^{10}	2.2×10^{5}	4500
cyclohexane	2.0	83 (49%), 220 (51%)	1.2×10^{10}, 4.5×10^{9}	1.6×10^{5}	6300
		Dyad **7**			
PhCN	25.9	45 (99%)	2.2×10^{10}	5.9×10^{9}	170
THF	7.5	24 (95%)	4.2×10^{10}	5.5×10^{9}	24
toluene	2.4	41 (95%)	2.2×10^{10}	6.4×10^{5}	1600
cyclohexane	2.0	40 (70%)	2.2×10^{10}	4.6×10^{5}	2200

[a] Determined from fluorescence lifetime measurements using eq 1. The lifetime of the reference corrole **4** was found to be 5.3, 4.7, 5.0, and 4.2 ns in cyclohexane, toluene, THF, and PhCN, respectively. [b] Determined from the decay of the fullerene radical anion band from the femto- and nanosecond transient absorption measurements.

triplet excited state of corrole. That is, during the charge recombination process, population of the triplet state is not favorable.

Kinetic information about the excited singlet-state quenching of corrole in the dyads was obtained from time-resolved fluorescence studies. As shown in Figure 4b,c, the emission decay could be curve-fitted to a biexponential function in both polar and nonpolar solvents. By assuming that the fast-decaying component is due to charge separation, the rate constant of charge separation (k_{CS}) was determined according to eq 1, and the data are listed in Table 2.

$$k_{CS} = (1/\tau_f)_{dyad} - (1/\tau_f)_{ref} \quad (1)$$

In agreement with the steady-state emission data, the quantum yield, Φ_{CS}, calculated according to eq 2 for charge separation was found to be >97% for the dyad in any of the studied solvents. The magnitude of k_{CS}, although very high, revealed a trend with respect to the solvent polarity. That is, the rates were found to be an order of magnitude higher in more polar solvents compared to those in the nonpolar solvents (Table 2).

$$\Phi_{CS} = [(1/\tau_f)_{dyad} - (1/\tau_f)_{ref}]/(1/\tau_f)_{dyad} \quad (2)$$

In order to unravel the mechanism of the quenching process, time-resolved transient absorption spectra of the dyads were obtained by femtosecond laser flash photolysis in deaerated solutions. The transient band observed around 1000 nm in all of the studied solvents was a clear indication of the formation of fulleropyrrolidine radical anion (Figure 5 and Figure S2 in the Supporting Information).[11]

The signal for the corrole cation radical, which is expected to appear around 670 nm, was obstructed by the strong bleaching of the visible bands of the corrole in the monitored wavelength region (see Figure S3 in the Supporting Information for the cation radical spectrum of corrole). In addition to the fulleropyrrolidine anion racial peak around 1000 nm, a new band at 1260 nm was also observed, corresponding to the singlet−singlet transition of the corrole. The decay of this band was accompanied by the rise of the fullerene anion radical band, suggesting electron transfer occurring from the singlet excited state of corrole in the dyad.

The rise in absorbance at 1000 nm due to the radical ion-pair corrole$^{\bullet+}$−$C_{60}^{\bullet-}$ (k_{CS}) is fitted well using the k_{CS} values determined by the fluorescence lifetime measurements, given in Table 1. The decay rate constants of the radical ion-pair corrole$^{\bullet+}$−$C_{60}^{\bullet-}$ (charge recombination rate constants, k_{CR}) were determined by using both femtosecond and nanosecond transient absorption methods. The nanosecond transient absorption spectra of the dyad in both benzonitrile and THF revealed no peak around 1000 nm corresponding to the fulleropyrrolidine anion formation, suggesting a very fast charge recombination process in polar solvent (see Supporting Information, Figure S4, for the spectra). In order to resolve this issue of obtaining the k_{CR} value in polar solvents, the decay in absorbance of the 1000 nm band in the femtosecond transient spectra was monitored in polar benzonitrile and THF (see Figure 5, lower panels), and the data thus obtained for the dyads are listed in Table 2. k_{CR} values on the order of 10^{10} s^{-1} were obtained, indicating a fast charge recombination process in polar solvents.

Interestingly, when nanosecond transient absorption of the dyad in nonpolar toluene and cyclohexane was monitored, a long-lived transient peak, on the order of several microseconds, was observed around 1000 nm, corresponding to fullerenepyrrolidine (Figure 6, upper panels). The k_{CR} value determined by monitoring the decay of this band (Figure 6, lower panels) was nearly 5 orders of magnitude smaller than that obtained in polar solvents (Table 2). It may be mentioned here that back electron transfer occurs in the radical ion-pair to produce the ground state rather than the triplet excited state of C_{60}, because the CS state energy is lower than the triplet energy of C_{60} (*vide supra*). In fact, no corrole or fullerene triplets were observed in spectra during the nanosecond laser flash photolysis measurements of the dyads in the studied solvents. The quantum yields of the CS state are determined to 0.88 ± 0.05 in toluene and 0.84 ± 0.05 in cyclohexane from the absorption of monofunctionalized fullerene at 1000 nm (ϵ_{1000} = 4700 M^{-1} cm^{-1}),[39] using the absorbance of the triplet−triplet absorption of free-base tetraphenylporphyrin (ϵ_{690} = 3500 M^{-1} cm^{-1}, $\Phi_{triplet}$ = 0.84 in toluene) as a reference.[40]

(39) (a) Imahori, H.; Tamaki, K.; Guldi, D. M.; Luo, C.; Fujitsuka, M.; Ito, O.; Sakata, Y.; Fukuzumi, S. *J. Am. Chem. Soc.* **2001**, *123*, 2607–2617. (b) Luo, C.; Fujitsuka, M.; Huang, C.-H.; Ito, O. *Phys. Chem. Chem. Phys.* **1999**, *1*, 2923–2928.

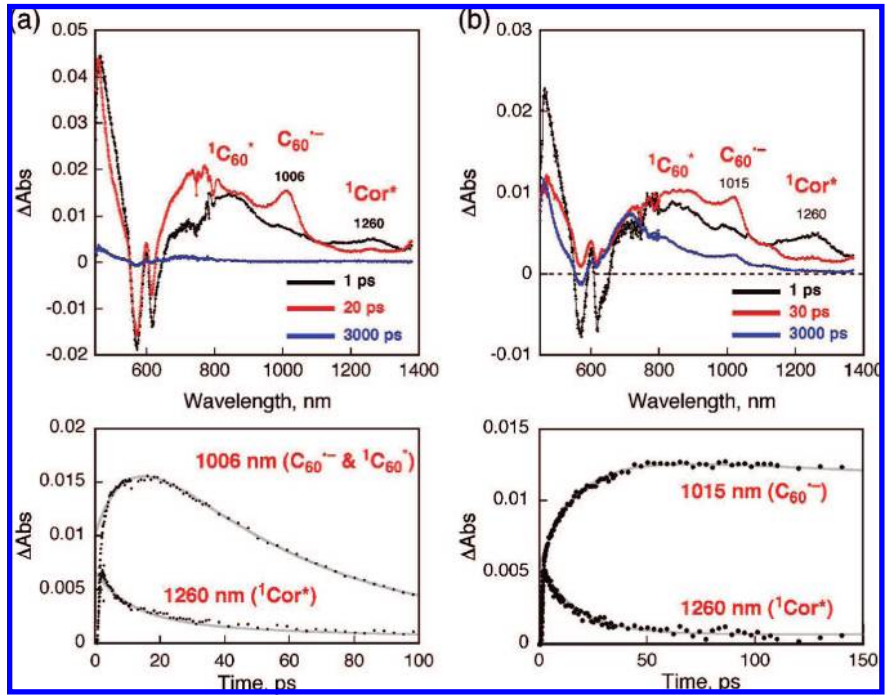

Figure 5. Femtosecond transient absorption spectra of dyad **6** in (a) benzonitrile and (b) toluene (top panel) after femtosecond laser pulse irradiation by the 410 nm laser at the indicated time intervals at 298 K. The time profiles of the fullerene anion radical at 1000 nm in benzonitrile and toluene are shown in the bottom panels, respectively. Solid curves represent the best fit to the two-exponential decay.

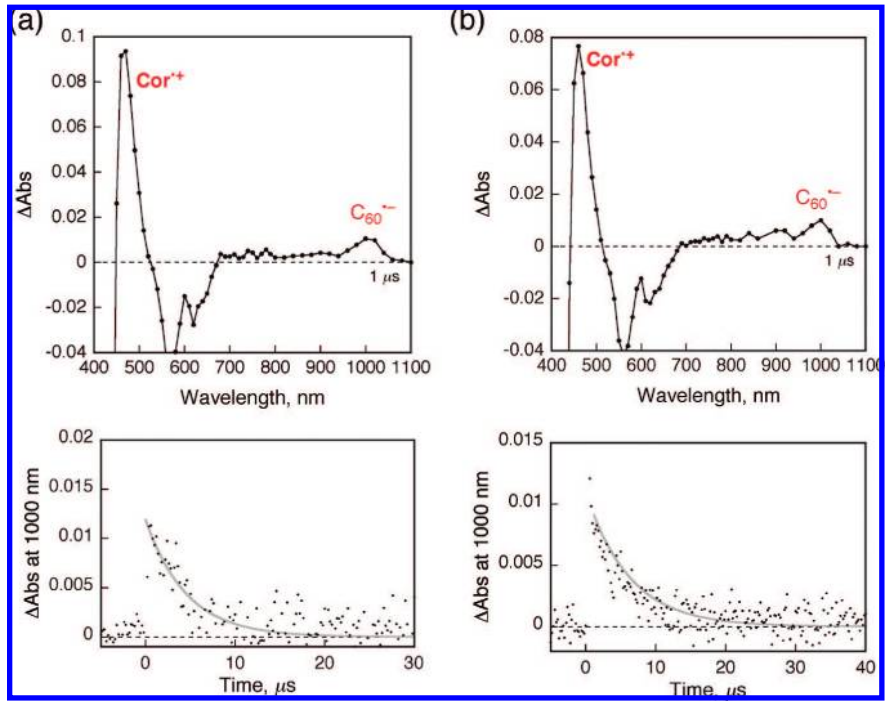

Figure 6. (Top) Nanosecond transient absorption spectra of the dyad **6** in (a) toluene and (b) cyclohexane irradiated by the 426 nm laser at 1 μs time intervals at 298 K. (Bottom) Time profiles of the fullerene radical anion at 1000 nm in toluene and cyclohexane, respectively. The solid curves represent the best fit to the single-exponential decay.

Kinetics Data Analysis: Marcus Plot. To quantify the driving force dependence on the electron-transfer rate constants (k_{ET}), eq 3 was employed:[22]

$$k_{ET} = \left(\frac{4\pi^3}{h^2\lambda k_B T}\right)^{1/2} V^2 \exp\left[-\frac{(\Delta G^0_{ET} + \lambda)^2}{4\lambda k_B T}\right] \qquad (3)$$

where V is the electronic coupling matrix element, k_B is the Boltzmann constant, $h$is the Planck constant, and T is the absolute temperature. Figure 7 shows the driving force dependence of log k_{ET} (k_{CS} and k_{CR}) for charge separation and charge recombination for dyad **6** in benzonitrile, THF, and toluene at 298 K.[41] The solid lines are drawn as the best-fit lines using the values of $\lambda = 0.76$ eV and $V = 20$ cm^{-1} for polar solvents

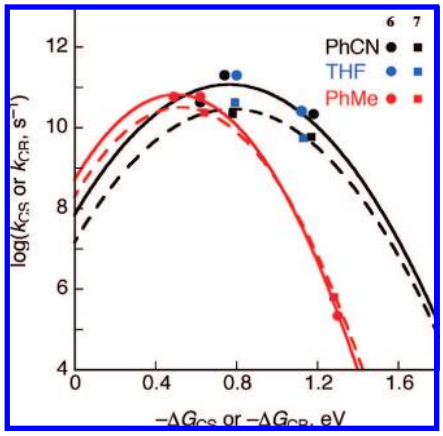

Figure 7. Marcus plots of log k_{CS} or k_{CR} vs $-\Delta G_{CS}$ or $-\Delta G_{CR}$ for photoinduced electron transfer and back electron transfer for dyads **6** (circles with solid lines) and **7** (squares with dashed lines) in polar (benzonitrile and THF, black and blue lines) and nonpolar (toluene, red lines) solvents at 298 K. The curves represent the best fit to eq 3, yielding the λ and V values shown in Table 3.

Table 3. Reorganization Energies of Electron Transfer (λ) and Electronic Coupling Terms (V) for the Corrole−Fullerene Dyads **6** and **7** in Different Polarity Solvents

solvent	λ, eV	V, cm^{-1}
	Dyad **6**	
polar[a]	0.76	20
nonpolar[b]	0.51	14
	Dyad **7**	
polar[a]	0.78	10
nonpolar[b]	0.53	9.5

[a] PhCN and THF. [b] Toluene.

(black, blue) and $\lambda = 0.51$ eV and $V = 14$ cm^{-1} for nonpolar solvent (red).

Similar analysis of the kinetic data for dyad **7** revealed values of $\lambda = 0.78$ eV and $V = 10$ cm^{-1} for polar solvents and $\lambda = 0.53$ eV and $V = 9.5$ cm^{-1} for nonpolar solvent. The increased λ and decreased V for **7** compared to **6** are consistent with an increased donor−acceptor distance of **7** due to the biphenyl spacer. The large V values for both dyads is consistent with the nearly adiabatic nature of the electron transfer between the free-base corrole and the C_{60} moieties in the dyads. Since the driving force of the charge recombination is larger than the λ value (0.51−0.78 eV), the charge recombination process lies deeply in the Marcus inverted region, where larger the driving force, the smaller is the electron-transfer rate constant. The values of λ and V are summarized in Table 3.

An energy level diagram showing the photochemical events in polar as well as nonpolar solvents for the corrole−fullerene dyads is presented in Figure 8. The energy of different states was calculated from the redox and emission data listed in Table 1. The triplet energy of corrole, obtained from low-temperature phosphorescence measurements, is close to that of porphyrin; however, owing to the easier oxidation and the ability to tune the macrocycle redox potential by placing appropriate electron-withdrawing substituents at the *meso*-positions of the corrole ring, it has been possible to position the CS energy level slightly

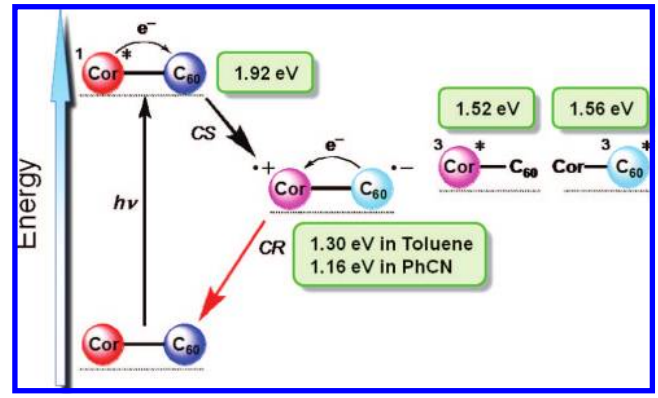

Figure 8. Energy level diagram depicting the photochemical events in polar and nonpolar solvents for the corrole−fullerene dyad **6**.

below the triplet energy level of either of the donor and acceptor entities for both polar and nonpolar solvent media. As a consequence of this and the discussions in the preceding paragraph, the much desired long-lived CS state has been achieved in the studied corrole−fullerene dyads in nonpolar solvents.

Conclusions

This work presents the first example of a tribasic corrole as an electron donor in a photosynthetic reaction center model system using fullerene as an electron acceptor. The donor corrole entity, owing to its facile oxidation compared to the traditionally used porphyrin analogues, yielded higher exothermicity for the light-induced charge separation process. Consequently, efficient charge separation was observed in the studied solvents from the time-resolved emission and femto- and nanosecond laser flash photolysis measurements. The charge recombination rates were found to be highly dependent on the solvent polarity. Due to the appropriate positioning of the energy levels of the CS state with respect to the triplet energy level and the small reorganization energies of electron transfer in nonpolar solvents, it was possible to achieve a radical ion-pair with the lifetime on the order of few microseconds in nonpolar solvents. This work, in addition to utilizing corrole as an electron donor for the first time, demonstrates the importance of positioning energy levels and small solvent reorganization energies in covalently linked donor−acceptor dyads to attain the long-lived CS state in nonpolar solvents.

Experimental Section

Chemicals. Buckminsterfullerene, C_{60} (+99.95%), was from SES Research, (Houston, TX). All the reagents were from Aldrich Chemicals (Milwaukee, WI), while the bulk solvents utilized in the syntheses were from Fischer Chemicals. Tetrabutylammonium perchlorate, (n-Bu_4N)ClO_4, used in the electrochemical studies was from Fluka Chemicals. Preparative-scale size exclusion chromatography (SEC) was performed using BioRad Bio-Beads SX-1 with THF as eluent. Tetrahexylammonium perchlorate, (n-Hex_4N)ClO_4, was synthesized according to the literature.[42] Dipyrromethane (**1**) was prepared according to the literature procedure.[43]

10-(4-Formylaryl)-5,15-bis(pentafluorophenyl)corrole (4 and 5 in Scheme 1). Pentafluorophenyl-dipyrromethane (**1**) (1.56 g, 5 mmol) and aldehydes **2** and **3** (2.5 mmol) were dissolved in MeOH

(40) (a) Pekkarinen, L.; Linschitz, H. *J. Am. Chem. Soc.* **1960**, *82*, 2407–2411. (b) Gratz, H.; Penzkofer, A. *Chem. Phys.* **2000**, *254*, 363–374.
(41) The driving force of electron transfer is given in Table 1, where the electrostatic term is neglected because positive and negative charges in the CS state are highly delocalized in the present system.
(42) Fukuzumi, S.; Ohkubo, K.; Suenobu, T.; Kato, K.; Fujitsuka, M.; Ito, O. *J. Am. Chem. Soc.* **2001**, *123*, 8459–8467.
(43) Laha, J. K.; Dhanalekshmi, S.; Taniguchi, M.; Ambroise, A.; Lindsey, J. S. *Org. Process Res. Dev.* **2003**, *7*, 799–812.

(250 mL). Concentrated HCl_{aq} (12.5 mL) in water (250 mL) was then added, and the resulting suspension was stirred at room temperature for 1 h. The reaction mixture was extracted with $CHCl_3$ (2 × 50 mL), and the organic phase was washed with water (3 × 50 mL), dried (Na_2SO_4), and concentrated to 40 mL volume. Dichlorodicyanoquinone (DDQ) (1.475 g, 6.5 mmol) was dissolved in toluene/CH_2Cl_2 (1:3, 40 mL), and both mixtures were added simultaneously to the vigorously stirred CH_2Cl_2 (50 mL). After 15 min, the reaction mixture was concentrated to one-fourth of the initial volume and filtered through a silica pad (CH_2Cl_2). The fluorescent band was collected, evaporated, and chromatographed (dry column vacuum chromatography,[44] silica, CH_2Cl_2/hexanes, 1:1). After evaporation, the residue was dissolved in THF and loaded on the SEC column (THF). The corrole fraction was collected, evaporated, and crystallized from $CHCl_3$/pentane to afford pure corrole as dark violet crystals (yield 30−38%).

4: $R_f = 0.32$ (CH_2Cl_2/hexanes, 3:2); ^{1}H NMR (500 MHz, $CDCl_3$) δ −3 to −1.5 (br s, 3H), 8.28, 8.37 (AA′BB′, $J = 7.9$ Hz, 2 × 2H, C_6H_4), 8.58 (br s, 2H, β-H), 8.65 (d, $J = 4.7$ Hz, 2H, β-H), 8.73 (d, $J = 4.6$ Hz, 2H, β-H), 9.13 (d, $J = 4.2$ Hz, 2H, β-H), 10.34 (s, 1H, CHO); EI-HR obsd 734.1183 [$M^{\bullet+}$], calcd exact mass 734.1163 ($C_{38}H_{16}N_4OF_{10}$); λ_{abs} (toluene, $\epsilon \times 10^3$, M^{-1} cm^{-1}) 424 (103), 568 (15. 6), 614 (8.56), 640 (4.55) nm. Anal. Calcd for $C_{38}H_{16}N_4OF_{10}$: C, 62.13; H, 2.20; N, 7.63. Found: C, 61.94; H, 2.32; N, 7.85.

5: ^{1}H NMR ($CDCl_3$) δ 9.11 (d, 2H, β-pyrrole *H*), 8.70−8.62 (m, 2H, β-pyrrole *H*), 8.60−8.54 (m, 4H, β-pyrrole *H*), 8.25−8.18 (m, 4H, phenyl *H*), 5.26 (s, 1H, pyrrolidine *H*), 5.10 (d, 1H, pyrrolidine *H*), 4.42 (d, 1H, pyrrolidine *H*), 3.14 (s, 3H, $-NCH_3$); UV−vis (toluene, nm) 310, 329, 416, 562.5, 615, 644.

Synthesis of the Corrole−Fullerene Dyads 6 and 7. 10-(4-Formylaryl)-5,15-bis(pentafluorophenyl)corrole (**4** and **5**) (0.14 mmol) and sarcosine (23 mg, 0.25 mmol) were added to a solution of C_{60} (44 mg, 0.06 mmol) in dry toluene (100 mL) and refluxed for 12 h. The progress of the reaction was monitored by using TLC every 1 h. After 12 h, the solvent was evaporated under vacuum, and the crude compound was purified on a silica gel column using hexanes/toluene (60:40 v/v). Evaporation of the solvent yielded the title compound as a greenish purple solid (yield ∼40%).

6: ^{1}H NMR ($CDCl_3$) δ 9.11 (d, 2H, β-pyrrole *H*), 8.70−8.62 (m, 2H, β-pyrrole *H*), 8.60−8.54 (m, 4H, β-pyrrole *H*), 8.25−8.19 (m, 4H, phenyl *H*), 5.26 (s, 1H, pyrrolidine *H*), 5.10 (d, 1H, pyrrolidine *H*), 4.42 (d, 1H, pyrrolidine *H*), 3.13 (s, 3H, $-NCH_3$); UV−vis (toluene, nm) 310, 329, 416, 562.5, 615, 644; MALDI-MS calcd 1481.16, found 1481.17.

7: ^{1}H NMR ($CDCl_3$) δ 9.12 (d, 2H, β-pyrrole *H*), 8.80−8.70 (m, 4H, β-pyrrole *H*), 8.58 (m, 2H, β-pyrrole *H*), 8.24 (d, 2H, biphenyl *H*), 7.90−8.10 (m, 6H, biphenyl *H*), 4.95−5.05 (m, 2H, pyrrolidine *H*), 4.26 (d, 1H, pyrrolidine *H*), 2.95 (s, 3H, $-NCH_3$); ESI mass (in CH_2Cl_2) calcd 1557.74, found 1557.2.

Instrumentation. ^{1}H NMR spectra were obtained from chloroform-d_1 solutions using a Varian 400 MHz NMR spectrometer with tetramethylsilane as internal standard. The UV−visible spectral measurements were carried out with a Shimadzu model 1600 UV−visible spectrophotometer. The fluorescence emission was monitored by using a Varian Eclipse spectrometer. Cyclic voltammograms were recorded on a EG&G P PARSTAT electrochemical analyzer using a three-electrode system. A platinum button electrode was used as the working electrode. A platinum wire served as the counter electrode, and Ag/AgCl was used as the reference electrode. Ferrocene/ferricenium redox couple was used as an internal standard. All the solutions were purged prior to electrochemical and spectral measurements using argon gas.

Theoretical Calculations. The computational calculations were performed by DFT B3LYP/3-21G(*) methods with the GAUSSIAN 03 software package[34] on high-speed computers. The molecular electrostatic potential maps and frontier orbitals were generated using the GaussView program.

Time-Resolved Fluorescence Absorption Measurements. Femtosecond fluorescence upconversion measurements were carried out using a Integra-C laser system and an optical detection system provided by Ultrafast Systems (Halcyone). The source for the excitation and gate pulses was derived from the fundamental output of the Integra-C laser system (780 nm, 2 mJ/pulse and fwhm = 130 fs) at a repetition rate of 1 kHz. The instrument allows the frequency mixing of incoherent fluorescence (resulting from exciting a sample with a short laser pulse) with a probe laser pulse (fwhm = 130 fs) in a nonlinear optical crystal. The optical setup is designed to work with a regeneratively amplified Ti-sapphire laser. The gate beam is sent through a computer-controlled optical delay stage and is focused on the nonlinear crystal, together with the fluorescence from the sample. The excitation pulse ($\lambda = 410$ nm) is sent through a half-wave plate/neutral density assembly and is focused on the sample. The excitation of the sample can be performed in transmissive (for clear samples) or reflective mode (for opaque samples). The resulting fluorescence is collected by an objective and, together with a gate beam, is sent to a nonlinear crystal. The upconverted fluorescence signal is collected after the crystal with an objective and sent through the set of filters and a monochromator for spectral purification. A photomultiplier tube and single photon counting unit are used to monitor the signal intensity.

Subpicosecond time-resolved fluorescence decays were measured by using a Photon Technology International GL-3300 instrument with a Photon Technology International GL-302 and a nitrogen laser/pumped dye laser system equipped with a four-channel digital delay/pulse generator (Standard Research System Inc. DG535) and a motor driver (Photon Technology International MD-5020). The excitation wavelength was 525 nm, using Coumarin 540A (Exciton Co., Ltd.).

Time-Resolved Transient Absorption Measurements. Femtosecond laser flash photolysis was conducted using a Integra-C laser system and an optical detection system provided by Ultrafast Systems (Helios). The source for the pump and probe pulses was derived from the fundamental output of the Integra-C laser system (780 nm, 2 mJ/pulse and fwhm = 130 fs) at a repetition rate of 1 kHz. A second harmonic generator introduced in the path of the laser beam provided 410 nm laser pulses for excitation. Here, 95% of the fundamental output of the laser was used to generate the second harmonic, while 5% of the deflected output was used for white light generation. Prior to generating the probe continuum, the laser pulse was fed to a delay line that provided an experimental time window of 3.2 ns with a maximum step resolution of 7 fs. The pump beam was attenuated at 5 μJ/pulse with a spot size of 2 mm diameter at the sample cell, where it was merged with the white probe pulse at a close angle (<10°). The probe beam, after passing through the 2 mm sample cell, was focused on a 200 μm fiber optic cable which was connected to a CCD spectrograph. Typically, 5000 excitation pulses were averaged to obtain the transient spectrum at a set delay time. The kinetic traces at appropriate wavelengths were assembled from the time-resolved spectral data.

Nanosecond time-resolved transient absorption measurements were carried out using the laser system provided by UNISOKU Co., Ltd. Measurements of nanosecond transient absorption spectrum were performed according to the following procedure. A deaerated solution containing a dyad was excited by a Panther OPO pumped by a Nd:YAG laser (Continuum SLII-10, 4−6 ns fwhm) at $\lambda = 430$ nm. The photodynamics were monitored by continuous exposure to a xenon lamp (150 W) as a probe light and a photomultiplier tube (Hamamatsu 2949) as a detector. Transient spectra were recorded using fresh solutions in each laser excitation. The solution was deoxygenated by argon purging for 15 min prior to measurements.

Acknowledgment. This work is supported by the National Science Foundation (CHE 0804015 to F.D.) and a Grant-in-Aid

(44) Pedersen, D. S.; Rosenbohm, C. *Synthesis* **2001**, 2431–2434.

(Nos. 19205019 and 19750034 to S.F. and K.O.) from the Ministry of Education, Culture, Sports, Science and Technology, Japan, and the Polish Ministry of Research and Higher Education.

Supporting Information Available: Optimized structure of **7**, optical spectra of the corrole cation generated by chemical oxidation, femtosecond transient absorption spectra of **6** in THF and cyclohexane, nanosecond transient absorption spectra of **6** in benzonitrile and THF, phosphorus spectrum of corrole **4**, nanosecond transient absorption spectrum of free-base corrole **4** in benzonitrile, and complete ref 34. This material is available free of charge via the Internet at http://pubs. acs.org.

JA804665Y